

**CORRELATION BETWEEN COHERENT STRUCTURES AND  
WALL SHEAR STRESS FLUCTUATIONS  
(SIMULTANEOUS MEASUREMENT OF VELOCITIES, WALL SHEAR STRESS  
AND FLOW VISUALIZATION)**

**Yoshio Furukawa**

Graduate school of Science and Engineering, Aoyama Gakuin, University  
Chitosedai 6-16-1, Setagaya-ku, Tokyo 153-8572, Japan

**Isao MISU, Nobumi SAIDA**

Department of Mechanical Engineering, Aoyama Gakuin University,  
Chitosedai 6-16-1, Setagaya-ku, Tokyo 153-8572, Japan

**ABSTRACT**

When studying organized motions in a turbulent wall flow, it is useful to clarify the relationship between organized motions and wall shear stress fluctuations. This is because the momentum transfer from the wall region to the outer region and vice versa causes wall shear stress fluctuations in a turbulent boundary layer. In past studies, the relationship between organized motions and wall shear stress fluctuations was investigated using a single hot wire (or array of hot wires) and a wall shear stress gage. However, the relationship between wall shear stress fluctuations and visualized flow pattern was not reported. In the present study, velocity and wall shear stress fluctuations were measured simultaneously and flow pattern was observed. In order to identify organized motions on the basis of wall shear stress fluctuations, a scheme for detecting the organized motions was used. This scheme detects the organized motions when the ratio of the amplitude of wall shear stress fluctuations to the standard deviation of the wall shear stress fluctuations (i.e. r.m.s. value) is greater or less than a threshold level. Experiments showed that ejection events detected using wall shear stress fluctuations with a threshold correspond to ejections identified using the side and top views of dye flow visualization. In addition sweep events detected using wall shear stress fluctuations with a threshold correspond to sweeps recognized using the end view of dye flow visualization.

**Nomenclature**

$L$  : Distance from starting point of the test section  
 $u$  : Velocity in boundary layer  
 $u_e$  : Velocity at the edge of boundary layer  
 $u_\tau$  : Friction velocity ( $(\bar{\tau}/\rho)^{1/2}$ )  
 $u'$  : Streamwise velocity fluctuation  
 $u_{rms}$  : Root-mean-square value of  $u'$   
 $u^+$  :  $u/u_\tau$   
 $v'$  : Velocity fluctuation normal to wall  
 $v_{rms}$  : Root-mean-square value of velocity  $v'$   
 $x, y, z$  : Coordinates of origin at flush-mounted hot film gage (see figure 1)  
 $y^+$  :  $yu_\tau/\nu$   
 $\nu$  : Kinematic viscosity of water  
 $\rho$  : Density of water  
 $\tau$  : Wall shear stress  
 $\bar{\tau}$  : Time averaged wall shear stress  
 $\tau'$  : Wall shear stress fluctuation  
 $\tau_{rms}$  : Root-mean-square value of  $\tau'$

**1. Introduction**

In experimental fluid dynamics, it is useful to define the relationship between wall shear stress fluctuations and organized motions in a turbulent wall flow. Previous studies concerning the relationship between wall shear stress and organized motions have been made by Brown et al.(1977), Misu et al. (1999) and Wietrzad et al.(1994). These investigations were concerned with the correlation of wall shear stress fluctuations and streamwise velocity fluctuations.

However, these investigations did not sufficiently clarify the relationship between wall shear stress fluctuations and organized motions. Kawahara et al.(1994) studied the relationship between wall shear stress fluctuations, obtained from the gradient of a velocity profile near the wall, and organized motions. In their study, Kawahara et al. focused on sweep events and did not discuss ejection events which are one of the turbulence production processes. The purpose of the present study is to examine the possibility of detecting the phase of the organized motion (i.e. ejection and sweep) using the wall shear stress fluctuations. For this purpose, velocities (streamwise and normal to the wall direction) and wall shear stress were measured simultaneously, and flow field visualization was performed.

## 2. Experimental apparatus

The experiment was conducted in an open recirculating water channel as shown in figure 1.

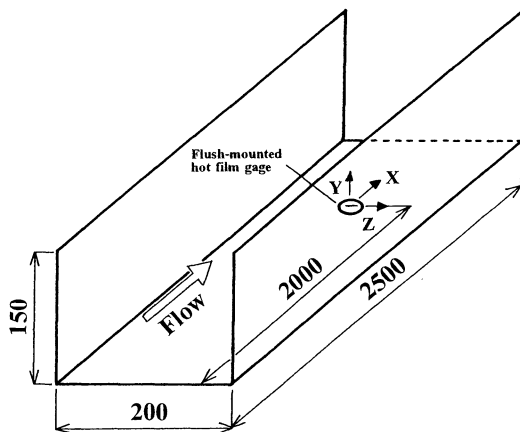


Figure 1. Schema of test-section

This open water channel has a test-section 2.5m long with a  $0.2 \times 0.1m^2$  cross sectional area. The measurements were carried out 2.0m downstream from the starting point of the test section. All measurements were performed under the Reynolds number,  $Re_L=3.5 \times 10^5$ , based on the velocity at the edge of the boundary layer  $u_\infty$  and the distance  $L$  measured from the starting point of the test section. In the present study, the main stream velocity was approximately  $0.177m/s$ . To obtain fully turbulent boundary layer flow, a tripping wire (3mm diameter) was set on the wall 50mm downstream from the starting point of the test section. For flow visualization, a fluorescent dye was introduced into the viscous sublayer through

0.5mm diameter holes which were bored into the wall 150mm and 135mm upstream from the measurement point. A laser light sheet probe (KANOMAX 1876) was used to illuminate the flow field. All visual data was recorded using a CCD video camera (SONY XC-77RR) and was stored in a laser video disk recorder (SONY LVR-3000AN). Wall shear stress measurements were made using a flush-mounted hot film gage (DANTEC 55R46 (Ni,  $0.75 \times 0.2mm$ ) connected to a constant temperature anemometer (KANOMAX 1013). In order to examine the relationship between the wall shear stress and the two velocity-components, a X-type hot film probe (TSI 1241-20W, diameter =  $50\mu m$  and sensing length of probe = 1mm), was also used at a height of  $y^+ = 30$ . The X-type hot film probe was connected to two constant temperature anemometer (KANOMAX 1013) / linearizer (KANOMAX 1011) pairs. Output signals from these linearizers were collected through a 12 bit AD converter. The sampling frequency was 40Hz and the total recording time was 300 seconds. Before flow visualization and simultaneous measurements of wall shear stress and velocities were performed, the velocity profile of the boundary layer was measured using a two dimensional LDV system. The measuring volume of the LDV system was approximately 0.1mm in diameter and 1.4mm in length. The measurements were performed with sampling rate of approximately 50Hz for 60 seconds.

In the present study, velocity at the edge of the boundary layer :  $u_e$  was  $17.7(cm/s)$ , kinematic viscosity :  $\nu$  was  $1.01 \times 10^{-2}(cm^2/s)$  and friction velocity :  $u_\tau$  was  $0.85(cm/s)$ , in which the friction velocity was determined using the Clauser chart.

## 3. Calibration method for the flush-mounted hot film gage

In the present study, a flush-mounted hot film gage was used in order to measure the wall shear stress. According to Liepman et al. (1954),  $\tau$  is proportional to  $Q_w^3$ , where  $Q_w$  is the heat transfer rate from the hot film to the fluid. If the flush-mounted hot film gage is connected to a constant temperature anemometer, the wall shear stress and the output voltage from the constant temperature anemometer are related as follows

$$\tau^{1/3} = AE^2 + B \dots \dots \dots (1)$$

where A and B are calibration constants. In the present study, the flush-mounted hot film gage

was calibrated over a period of two days. This period was chosen based on the experience of wind tunnel experiments where calibration constants changed daily. The calibration was made by determining the skin friction using the Clauser chart. A least square fit of 22 points was adopted to determine A and B. The calibration line and the measured data are shown in figure 2. As can be seen in figure 2, there is some degree of scatter and so  $E_0$  was also considered.  $E_0$  is the output voltage from the constant temperature anemometer when there is no convection over the hot film gage.  $E_0$  is related to the thermal conduction to a base substance and thermal radiation from the flush-mounted hot film gage.

Here, equation (1) is modified to

$$\tau^{1/3} = A'(E^2 - E_0^2) + B' \dots \dots \dots (2)$$

Figure 3 shows the new calibration line and data when  $E_0$  is considered. The data in figure 3 shows less scatter than the data in figure 2. As a result, equation (2) was used for the calibration equation. This calibration equation was established by Misu-Furukawa(1999). In figures 2 and 3, the dotted lines represent the mean  $\pm\sigma$ , where  $\sigma$  is the standard deviation.

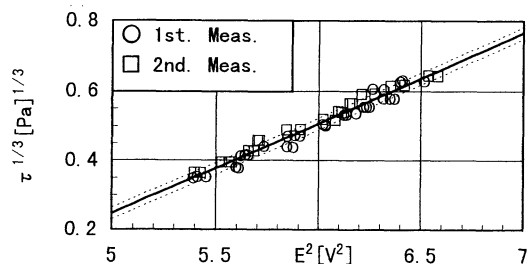


Figure 2. Calibration line without considering  $E_0$

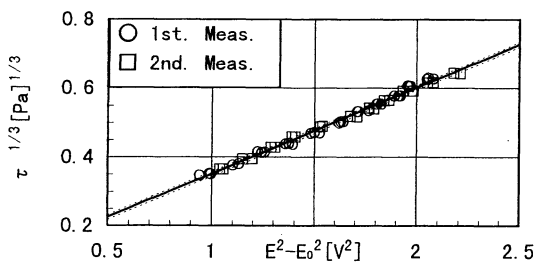


Figure 3. Calibration line considering  $E_0$

#### 4. Time averaged properties

Figure 4 shows the logarithmic time averaged velocity profile and figure 5 shows the distribution of the velocity fluctuations. In figure 4, the open circles represent time averaged streamwise

velocities obtained using the LDV and the solid circle represents time averaged streamwise velocity obtained using the X-type hot film probe. In figure 5, the open circles and open triangles represent root-mean-square values of streamwise and wall normal direction velocity fluctuations, obtained using the LDV, and the solid circle and the solid triangle represent values obtained using the X-type hot film probe. The results obtained using the LDV in figure 4 are in good agreement with Patel(1965)'s empirical formula  $u^+ = 5.5 \log_{10} y^+ + 5.45$ . The boundary layer flow was found to be a fully developed turbulent. The measurements using the X-type hot film probe were performed while fluorescent dye was being introduced into the viscous sublayer through small holes. As the results obtained using the X-type probe agree with the results obtained using the LDV, introducing fluorescent dye into the viscous sublayer did not disturb the flow.

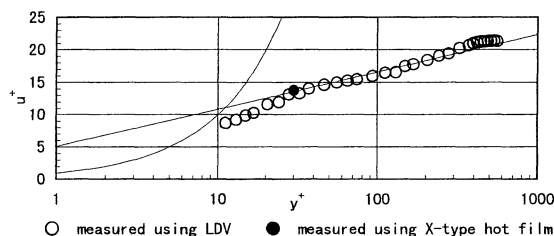


Figure 4.. Logarithmic time averaged velocity profile

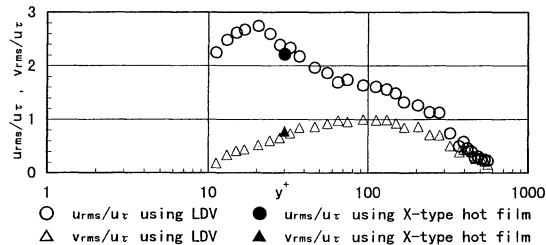


Figure 5. Distribution of velocity fluctuations

#### 5. Identification of ejection events using wall shear stress fluctuations

The ejection events must be identified using the visualization pictures in order to be correspondent to the ejection events detected using the wall shear stress fluctuations. Initially, the ejection events are identified using the side and top view sequences of the dye visualizations. The side view sequence is used to identify dye-marked fluid lifted up near the wall. The top viewing is used to identify dye-marked fluid passing the neighbor-

hood of the flush-mounted hot film gage. In the analysis of the flow visualization, an individual ejection event is identified using criteria similar to those used by Bogard et al.(1986) and Kawahara et al.(1995). An ejection event is defined as follows:

- 1) a dye-marked fluid initiates within  $\Delta x^+ = 300$  upstream from the position of the flush-mounted hot film gage,
- 2) its vertical motion is beyond  $y^+ = 30$ ,
- 3) it passes within  $\Delta z^+ = \pm 25$  of the flush-mounted hot film gage.

In order to record the side and top view sequences, a laser sheet approximately 20mm wide is used. A typical ejection process is shown in figure 6.

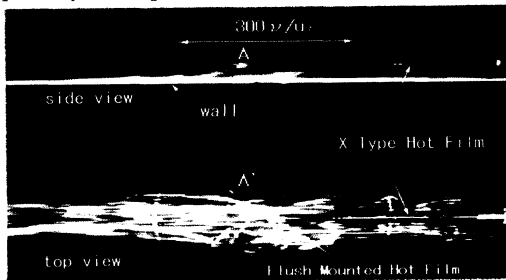


Figure 6-1.  $\Delta t = 0$

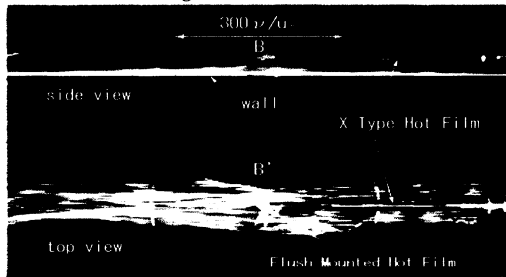


Figure 6-2.  $\Delta t = 4.9\nu/u_\tau^2$

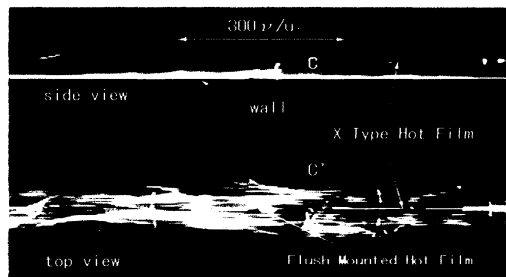


Figure 6-3.  $\Delta t = 9.8\nu/u_\tau^2$

Figure 6. Typical ejection event

Figure 6-1 shows dye-marked fluid that starts to lift up at the upstream of the flush-mounted hot film gage (character A). Figure 6-2 shows dye-marked fluid that passes the neighborhood of the X-type hot film located at  $y^+ = 30$  (character B) and passes within the  $\Delta z^+ = \pm 25$  region of the

flush-mounted hot film gage. Figure 6-3 shows dye-marked fluid that lifts beyond  $y^+ = 30$  and begins to diffuse (character C). Figure 7 shows example waveforms of  $u'$ ,  $v'$  and  $\tau'$  when the ejection event is occurring. In figure 7, characters A, B and C correspond to those in figures 6-1, 6-2 and 6-3 respectively.

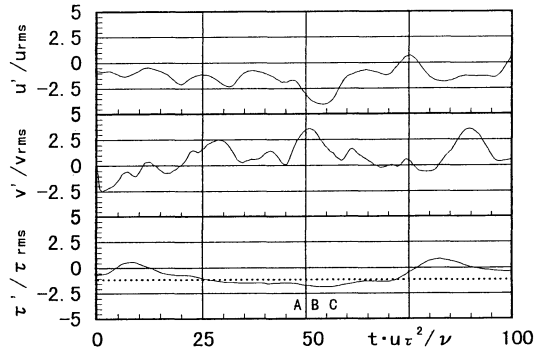


Figure 7. Example waveforms (ejection)

To identify ejection events using wall shear stress fluctuations, a conditional sampling technique is assumed as follows:

$$\tau'/\tau_{rms} < L_E \dots\dots\dots (3)$$

where,  $L_E$  is threshold level. The threshold level is determined when the rate at which ejections detected using wall shear stress fluctuations and those detected using visualized pictures are simultaneously identified is a maximum value. When  $L_E = -1.1$ , the identification rate for ejections is a maximum = 40%.

Figure 8 shows the conditionally averaged velocities and wall shear stress waveforms centered on the middle position of ejection events .

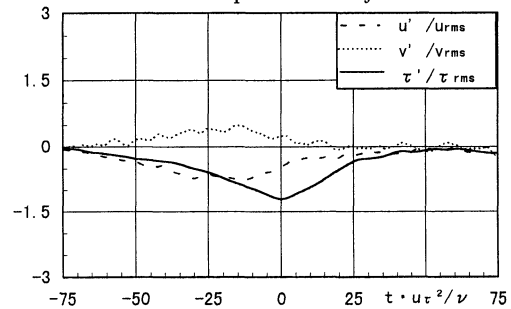


Figure 8. Conditionally averaged velocities and wall shear stress waveform

After low speed fluid has passed, the wall shear stress fluctuating component is less than zero, the streamwise velocity fluctuation component is less than zero and the velocity fluctuation component normal to the wall is greater than zero. Such flow

motion is ejection. From figure 8, it is seen that the ejection event continues for approximately 100 units on the viscous time scale.

### 6. Identification of sweep events using wall shear stress fluctuations

In order to identify sweep events by flow visualization, pictures of dye flow taken from downstream are used. By using these pictures, it is possible to grasp the flow toward the wall induced by longitudinal vortices in the wall vicinity. A laser sheet is illuminated from the upper position above the flush-mounted hot film gage. The streamwise thickness of the laser sheet is approximately 2mm. A typical sweep process is shown in figures 9-1 to 9-3. An arrow indicates the position of the flush-mounted hot film gage. Figure 9-1 shows two longitudinal vortices beginning to form. The vortex on the right side can be seen clearly in figure 9-2. In figure 9-3, the vortex on the right side has become unclear but the vortex on the left side starts to become clear.

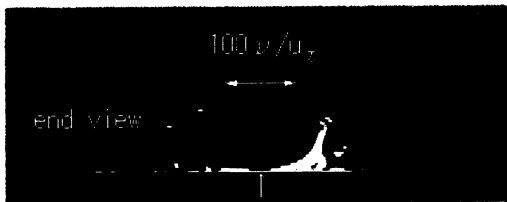


Figure 9-1.  $\Delta t = 0$

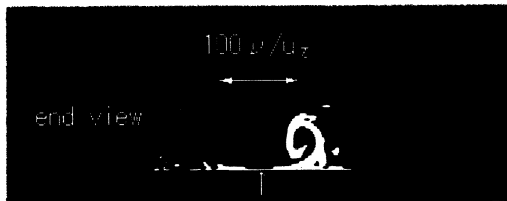


Figure 9-2.  $\Delta t = 4.9\nu/u_\tau^2$

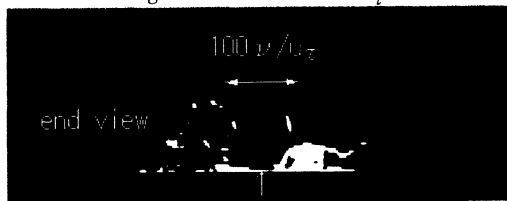


Figure 9-3.  $\Delta t = 9.8\nu/u_\tau^2$

Figure 9. Typical sweep event

Figure 10 shows example waveforms when the sweep event is occurring. In figure 10, the characters D, E and F correspond to the sequence from figure 9-1 to 9-3, respectively.

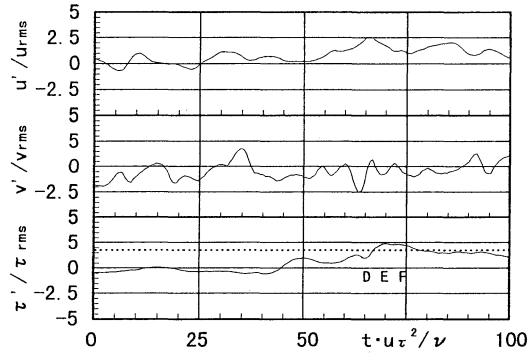


Figure 10. Example waveforms (sweep)

In order to identify sweep events using wall shear stress fluctuations, a conditional sampling technique is assumed as follows:

$$\tau' / \tau_{rms} > L_S \dots\dots\dots (4)$$

where,  $L_S$  is threshold level. The threshold level is determined when the rate at which the sweep detected using wall shear stress fluctuations and the sweep detected using flow visualized pictures are simultaneously identified is a maximum value. When  $L_S = 1.8$ , the identification rate for sweeps is a maximum value = 73%.

Figure 11 shows the conditionally averaged velocities and wall shear stress waveforms centered on the middle position of sweep events.

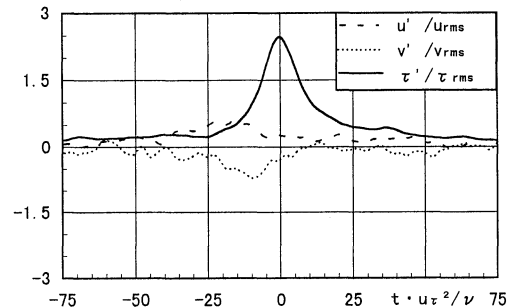


Figure 11. Conditionally averaged velocities and wall shear stress waveform

The wall shear stress fluctuations are greater than zero, because the high-speed fluid moves into the wall region during the sweep event. The streamwise velocity fluctuation component is greater than zero and the velocity fluctuation component normal to the wall is less than zero. Comparing figure 8 with figure 11, the duration of the sweep events is approximately 50 units on the viscous time scale, that is the duration of a sweep event is much shorter than that of an ejection event, and a sweep event consists of relatively short motions.

In figure 11, a time lag can be seen between the peak of  $u'/u_{rms}$  and  $v'/v_{rms}$ . If the structure which induced the sweep event passes parallel to the wall over the flush-mounted hot film gage, a time lag should not be seen. Therefore, the structure itself flows toward the wall region from the oblique upper region, because the peak of  $v'/v_{rms}$  follows the peak of  $u'/u_{rms}$ . In order to explain the structure moving down to the wall region, visualization pictures of a sweep event identified using wall shear stress fluctuation are shown in figures 12-1 to 12-3. In these pictures, it can be seen that dye-marked fluid (characters G, H and I) moving down the wall. Since the dye-marked fluid moves with the flow structure, figure 12 shows that the structure, which moves down the wall, induces the sweep event.

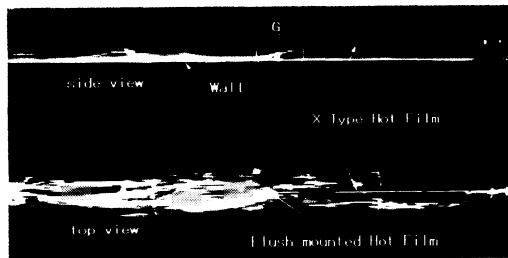


Figure 12-1.  $\Delta t = 0$

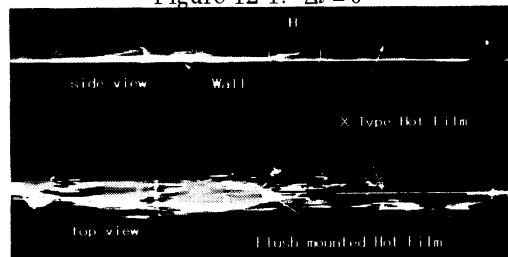


Figure 12-2.  $\Delta t = 4.9\nu/u\tau^2$

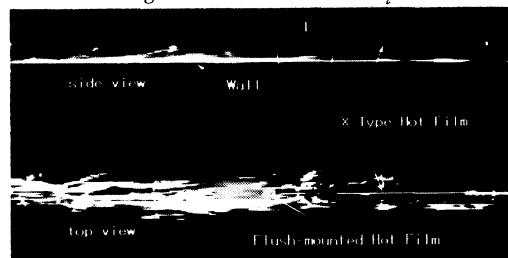


Figure 12-3.  $\Delta t = 9.8\nu/u\tau^2$

Figure 12. Typical sweep event (side and top view)

## 7. Conclusions

- (1) The calibrations show that  $\tau^{1/3}$  is proportional to  $E^2 - E_0^2$  which is better than  $E^2$  for water tunnel experiments.
- (2) Ejection events detected using wall shear

stress fluctuations with a threshold correspond to ejections identified using the side and top views of the dye flow visualization.

- (3) Sweep events detected using wall shear stress fluctuations with a threshold correspond to sweeps recognized using the end view of the dye flow visualization.
- (4) Ejection and sweep events detected using wall shear stress fluctuations correspond to ejection and sweep events identified using velocities fluctuations.

## Acknowledgments

The authors would like to thank Mr. Atushi Sato and Mr. Koji Nomura who helped in this investigation.

## REFERENCES

- Bogard, D. G. & Tiederman, W. G., 1986, "Burst detection with singlepoint velocity measurements", *J. Fluid Mech.* 179, pp.389-413
- Brown, G.L. & W. Thomas, A.S., 1977, "Large structure in a turbulent boundary layer", *Phys. Fluid* 20, pp.243-252
- Kawahara, G., Ayukawa, K., Ochi, J. & Ono, F., 1994, "Bursting Phenomena in a Turbulent Square-Duct Flow (Generation Mechanics of Turbulent Wall Shear Skin Friction)", *Trans. Japan Soc. Mech. Eng.*, 61-592 B, pp.4297-4304 (in Japanese)
- Liepman, H. W. & Skinner, G. T., 1954, "Shearing-stress measurements by use of a heated element", TN 3268
- Misu, I., & Furukawa, Y., 1999, "An improvement of calibration formula of a hot-film gage on measuring the wall shear stress in turbulent boundary layers", (to appear in), *Trans. Japan Soc. Mech. Eng.*, (in Japanese)
- Misu, I., Saida, N. & Yatabe, T., 1999, "Correlation between velocities and wall shear stresses in the bursting under favorable pressure gradients", (to appear in), *Trans. Japan Soc. Mech. Eng.*, (in Japanese)
- Patel, V.C., 1965, "Calibration of the Preston tube and limitations on its use in pressure gradients", *J. Fluid Mech.*, vol.23, pp.185-208
- Wietrzak, A. & Lueptow, R.M., 1994, "Wall shear stress and velocity in a turbulent axisymmetric boundary layer", *J. Fluid Mech.* 259, pp.191-218